AGU PUBLICATIONS

Water Resources Research

RESEARCH ARTICLE
10.1002/2015WR018076

Relation between grid, channel, and Peano networks in high-resolution digital elevation models

Samuele De Bartolo[1], Francesco Dell'Accio[2], Giuseppe Frandina[1], Giovanni Moretti[3], Stefano Orlandini[3], and Massimo Veltri[1]

[1]Dipartimento di Ingegneria Civile, Università della Calabria, Rende, Italy, [2]Dipartimento di Matematica e Informatica, Università della Calabria, Rende, Italy, [3]Dipartimento di Ingegneria Enzo Ferrari, Università degli Studi di Modena e Reggio Emilia, Modena, Italy

Key Points:
- Average junction degrees of real networks are modeled by perturbing the base case of the Peano network
- Estimated values of the perturbation parameter indicate the degrees of topological similarity between real and Peano networks
- Drainage densities of real and Peano networks match only for specific grid cell sizes and thresholds for channel initiation

Correspondence to:
S. De Bartolo,
samuele.debartolo@unical.it

Citation:
De Bartolo, S., F. Dell'Accio, G. Frandina, G. Moretti, S. Orlandini, and M. Veltri (2016), Relation between grid, channel, and Peano networks in high-resolution digital elevation models, *Water Resour. Res.*, *52*, 3527–3546, doi:10.1002/2015WR018076.

Received 7 SEP 2015
Accepted 13 APR 2016
Accepted article online 20 APR 2016
Published online 7 MAY 2016

Abstract The topological interconnection between grid, channel, and Peano networks is investigated by extracting grid and channel networks from high-resolution digital elevation models of real drainage basins, and by using a perturbed form of the equation describing how the average junction degree varies with Horton-Strahler order in Peano networks. The perturbed equation is used to fit the data observed over the Hortonian substructures of real networks. The perturbation parameter, denoted as "uniformity factor," is shown to indicate the degree of topological similarity between Hortonian and Peano networks. The sensitivities of computed uniformity factors and drainage densities to grid cell size and selected threshold for channel initiation are evaluated. While the topological relation between real and Peano networks may not vary significantly with grid cell size, these networks are found to exhibit the same drainage density only for specific grid cell sizes, which may depend on the selected threshold for channel initiation.

1. Introduction

The importance of investigating the relations between real channel networks and theoretical network models has been extensively recognized in the literature [e.g., *Howard*, 1990; *Willgoose et al*., 1991a,b,c,d; *Kirchner*, 1993; *Rodriguez-Iturbe and Rinaldo*, 1997; *Rinaldo et al*., 2006; *Perron et al*., 2012]. The theory of networks offers a way to study complex natural structures [*Albert and Barabási*, 2002; *Newman*, 2003]. The application of this theory to fluvial hydrology and geomorphology allows us to define channel networks as systems with a low degree of junction [*De Bartolo et al*., 2009]. This helps shaping our understanding of the mechanisms that control the dynamics and evolution of natural channel networks [*Perron et al*., 2012]. The application of the theory of networks to fluvial hydrology and geomorphology is grounded on the assumption that a channel network is a typical topological structure [*Shreve*, 1967], where junction nodes are not located randomly but are rather the result of relevant geophysical processes [*Kirchner*, 1993; *Perron et al*., 2012]. Under this assumption, the investigation of the mathematical laws describing the topology of junctions represents an effective way to identify and characterize the essential features of complex geophysical processes that underlie the formation of the channel network. Some researchers have argued that a misleading comparison between real and synthetic networks may arise from the correspondence of topological measures based on Horton's ratios [*Horton*, 1932, 1945; *Strahler*, 1952, 1957, 1958] or Tokunaga's matrices [*Kirchner*, 1993; *Rinaldo et al*., 2006]. However, recent literature based on the *Horton*-Strahler ordering remarks the effectiveness of the mathematical properties of river networks, which provide important insights for understanding fluvial landscape processes and evolution [e.g., *Perron et al*., 2012].

Several investigations have been carried out to characterize relevant morphometric parameters of complex drainage basins by means of simple and multiscaling relationships of Horton's indices [e.g., *Tarboton et al*., 1988; *La Barbera and Rosso*, 1989; *Marani et al*., 1991; *Rinaldo et al*., 1992; *Rigon et al*., 1993; *Rodriguez-Iturbe and Rinaldo*, 1997; *De Bartolo et al*., 2000, 2004, 2006a, 2006b; *Gaudio et al*., 2006]. The Peano network is often the key element for developing such investigations [*Mandelbrot*, 1977; *Marani et al*., 1991; *Flammini and Colaiori*, 1996; *Troutman and Over*, 2001; *Veitzer and Gupta*, 2001; *Tay et al*., 2006]. The Peano network is a deterministic, plane-filling fractal structure [*Marani et al*., 1991]. This structure can be easily generated through an iterative algorithm in which the numbers of interior and exterior nodes of the network are computed from geometrical series expansions by following strictly the Horton-Strahler hierarchy [*De Bartolo*

et al., 2009]. Owing to this similarity, the Peano network has also been adopted to predict the role of hydrologic controls on the ecological corridors in which the reaction and transport parts can be represented by nodes and links, respectively [*Campos et al*., 2006; *Bertuzzo et al*., 2007, 2008, 2010]. As pointed out by *Rinaldo et al*. [1998], since topological properties are partial descriptors of channel networks, Peano networks can only be used to solve network problems, like those connected to biological invasions, in which topology is the key determinant.

The concept of average junction degree to a given order introduced by *De Bartolo et al*. [2009] can be readily incorporated into hydrological, geomorphological, and biodiversity models to provide an objective topological descriptor for the considered channel network. More specifically, the perturbation of the law expressing the average junction degree of all substructures in the Peano network yields a suitable analytical model of the Hortonian substructures that can be observed in real channel networks [*De Bartolo et al*., 2009]. A first attempt to relate real and Peano networks was performed in *De Bartolo et al*. [2009] by considering the river network of the Corace River drainage basin, Italy, extracted from cartographic blue lines. The Peano network was found to represent the real channel network in terms of average junction degree by displaying relative errors on the order of 10^{-3}. The results of the study reported in *De Bartolo et al*. [2009] suggest therefore a more comprehensive analysis based on high-resolution topographic data and advanced terrain analysis methods that have recently become available [e.g., *Orlandini et al*., 2003, 2014].

In the present study, high-resolution digital elevation models (DEMs) of eight drainage basins located in four different geographical areas have been considered. For each drainage basin, the slope line network is extracted from DEM data by using the D8-LTD method [*Orlandini et al*., 2003; *Orlandini and Moretti*, 2009; *Orlandini et al*., 2014]. Within these slope line networks, the grid networks and the channel networks are distinguished and treated separately. The grid network is composed of all the slope lines connecting the DEM cell centers and extend therefore along both the hillslope and channel systems. The channel network is determined by predicting the channel heads along the slope line network and assuming that only the slope lines extending downslope the channel heads contribute to the channel network. Channel heads are predicted by using three threshold quantities, namely the drainage area A [*O'Callaghan and Mark*, 1984; *Tarboton*, 1997], a monomial function AS^2 of the drainage area A, and the local slope S [*Montgomery and Dietrich*, 1988], and the Horton-Strahler order ω^* of slope lines [*Peckham*, 1995a,b; *Orlandini et al*., 2011]. More than one thousand network substructures have been examined in the present study. A coarse graining analysis has been performed to investigate the role of grid cell size in the extraction of both grid and channel networks. The sensitivity of computed drainage density to grid cell size and channel initiation thresholds is also investigated to demonstrate the impact of these quantities in drainage basin hydrology.

2. Background

2.1. Average Junction Degree of Hortonian Networks

Channel networks are usually ordered according to the Horton-Strahler hierarchy [*Horton*, 1932, 1945; *Strahler*, 1952, 1957, 1958]. This hierarchy states that source streams are first order streams and that the order ω of a stream which originates from the junction of two streams of order l and k with $l, k \geq 1$ is given by

$$\omega = \max(l, k) + \delta_{lk}, \tag{1}$$

where δ_{lk} is the Kronecker delta [*Dodds and Rothman*, 1999]. A channel network is a graph that contains no cycles where the edges are streams and the nodes are junctions. In this configuration, it is possible to define the junction degree of a node, k_n, as the number of its inflow and outflow tributaries. In *Horton*ian networks, this number is equal to 1 for the exterior (source) and outlet nodes and it is on average equal to 3 or more for the interior nodes. Junction degrees higher than 3 can be due to the presence of fractures or junction faults that increase the number of tributary streams to a same junction. Once the junction degree of a node is defined locally, it is possible to define the total junction degree of a network, $\mathcal{K}$, that is the sum of the junction degrees computed over all n nodes. The average junction degree $\langle k_n \rangle$ is defined by the ratio

$$\langle k_n \rangle = \frac{\mathcal{K}}{n}. \tag{2}$$

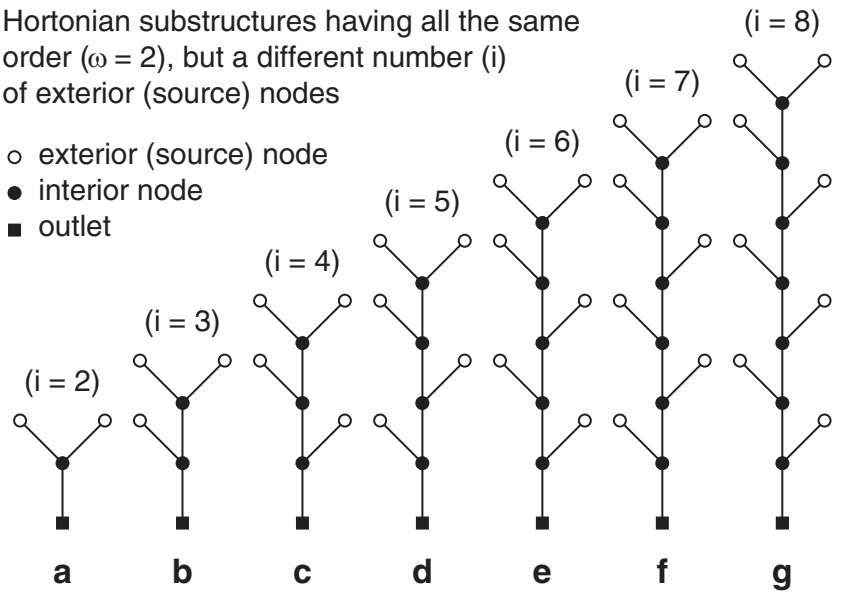

Figure 1. Sketch of eight Hortonian substructures of the second-order ($\omega = 2$) displaying a different number i of exterior (source) nodes. The substructure with $i = 2$ reported in Figure 1a represents the minimal configuration for a Hortonian substructure of order $\omega = 2$.

In the definition of the average junction degree, the meaning of "degree" is consistent with the terminology used by *Albert and Barabási* [2002] and *Newman* [2003], and must not be confused with the "junction angle" discussed by *Horton* [1932, 1945] and, more recently, by *Howard* [1971, 1990].

In the graph that represents the channel network ordered according to the *Horton*-Strahler ordering scheme, we can identify subsets of connected streams which are maximal with respect to the property that each stream is of order not greater than ω. These subsets are denoted as substructures of order ω. For each substructure of order ω, we can count the number i of its source nodes (the channel heads) and then compute the average junction degree of the substructure as

$$\langle k_n \rangle = \frac{2i-1}{i} \tag{3}$$

[*De Bartolo et al*., 2009]. It can be shown that the average junction degree, $\langle k_n \rangle$, can vary for each substructures of the same ω order and for i source nodes. For instance, seven substructures of the second-order ($\omega = 2$) displaying a different number i of source nodes, ranging from 2 to 8, are shown in Figure 1. The graph with $i = 2$ represents the minimal network structure (Figure 1a). In these cases, where $\omega = 2$, $\langle k_n \rangle$ ranges between 1.5 and 1.875 (Figures 1a and 1g, respectively). It can be verified that in the case of large trees characterized by a very high number of nodes, $\langle k_n \rangle$ approaches 2 [*Albert and Barabási*, 2002; *De Bartolo et al*., 2009]. The average junction degree $\langle k_n \rangle$ can be used to compare networks having the same order. It is specified here that the value of $\langle k_n \rangle$ computed over a network having order Ω cannot be used singly to evaluate the internal topological properties of the network. In fact, $\langle k_n \rangle$ is a global descriptor which may display comparable values for different networks. Hence, $\langle k_n \rangle$ can be used singly to only indicate topological dissimilarity. The internal topological properties of the network are, however, indicated by the variation of the average junction degrees $\langle k_n \rangle$ over all the substructure having orders $\omega = 1, \ldots, \Omega$. This variation may be represented by a single parameter as reported in section 2.3. In addition, as noted by *Rinaldo et al*. [1998], topologically similar networks may not play a comparable role in the description of all flow and transport processes. Under this light, it is acknowledged here that the average junction degree and the derived topological descriptors should be used as indicators of network topological similarity/dissimilarity or, in the broadest sense, of network dissimilarity only.

The variation of the average junction degree $\langle k_n(\omega) \rangle$ across all the channel network substructures, from the first-order ($\omega = 1$) to the maximum order ($\omega = \Omega$), provides an objective topological characterization of the entire channel network. This characterization can be synthesized by interpolating the values of $\langle k_n(\omega) \rangle$

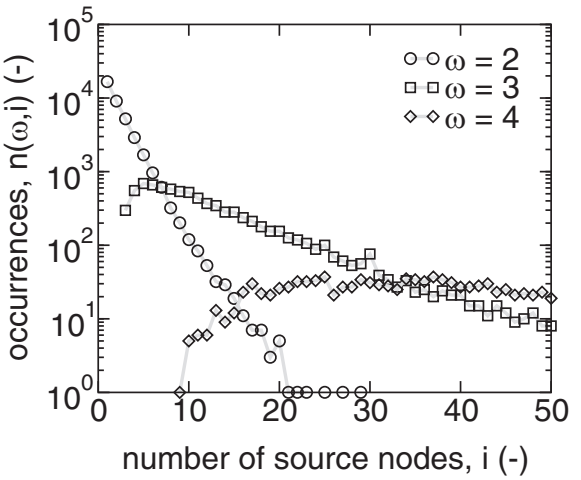

Figure 2. Occurrences of Hortonian substructures $n(\omega, i)$ having order ω ($\omega = 2, 3, 4$) and i exterior (source) nodes ($1 \le i \le 50$). These occurrences are computed by using, for instance, the 1 m digital elevation model of the real drainage basin RC3 introduced in section 3 (Figure 6) and the orders $\omega = 2, 3, 4$.

computed numerically with a functional relationship. This relationship, as we shall see in section 2.2, can be reduced to a form having an unique uniformity parameter. In general, the average junction degree of the channel network to the order $\omega = 1, \ldots, \Omega$ is given by the equation

$$\langle k_n(\omega) \rangle = \frac{\sum_{i=2^{\omega-1}}^{2^{\omega-1}+L-1} n(\omega, i) \frac{2i-1}{i}}{\sum_{i=2^{\omega-1}}^{2^{\omega-1}+L-1} n(\omega, i)}, \quad (4)$$

where $n(\omega, i)$ denotes the number of all substructures of order ω with i source nodes [*De Bartolo et al.*, 2009]. For each fixed order ω, the number i varies from $2^{\omega-1}$ to $2^{\omega-1}+L-1$, where L is the length of the vector of occurrences

$$\begin{gathered} \mathbf{n}(\omega) = [n(\omega, 2^{\omega-1}), n(\omega, 2^{\omega-1}+1), \ldots, n(\omega, 2^{\omega-1}+L-1)], \\ n(\omega, 2^{\omega-1}+L-1) \neq 0, \\ \text{and} \\ n(\omega, j) = 0, \end{gathered} \quad (5)$$

for any $j \ge 2^{\omega-1}+L$. In the definition of $\mathbf{n}(\omega)$, the values $n(\omega, i)$ as well as the values $n(\omega, j)$ do not appear since they are all vanishing. The quantities $n(\omega, i)$ display different behaviors for different orders ω. As shown for instance in Figure 2, for $\omega = 2$, $n(2, i)$ displays a decreasing exponential trend. For $\omega = 3$, $n(3, i)$ shows an unimodal trend limited to a narrow range of i, whereas for $\omega \ge 4$, $n(\omega, i)$ displays an unpredictable behavior (Figure 2). It is important to note that $\langle k_n(\Omega) \rangle = \langle k_n \rangle$ due to the requirement of maximality in the definition of substructures and for each $\omega = 1, \ldots, \Omega$, $\langle k_n(\omega) \rangle$ is a rational number.

A topological characterization of a channel network having order Ω can be provided by computing the average junction degrees $\langle k_n(\omega) \rangle$ of all the network substructures having orders $\omega = 1, \ldots, \Omega$ through equation (4). A single parameter can be used to represent the variation of $\langle k_n \rangle$ over these substructures as reported in section 2.3. The discriminatory power of $\langle k_n \rangle$ can be found in the preasymptotic range, that is for moderate values of the order ω, where $\langle k_n(\omega) \rangle$ belongs to the range

$$\frac{2 \times 2^{\omega-1} - 1}{2^{\omega-1}} \le \langle k_n(\omega) \rangle < 2. \quad (6)$$

Two fundamental features of the discrete function (4) are (1) the initial condition given by $\langle k_n(1) \rangle = 1$ and (2) the asymptotic condition given by $\lim_{\omega \to \infty} \langle k_n(\omega) \rangle = 2$. More details on the asymptotic properties of $\langle k_n(\omega) \rangle$ can be found in *De Bartolo et al*. [2009].

2.2. Average Junction Degree of the Peano Network

The Peano network is a deterministic plane-filling network with fractal dimension equal to 2 [*Mandelbrot*, 1977; *Dekking*, 1991]. The Peano network has been extensively studied by hydrologists. *Marani et al*. [1991] have shown analytically that the width function of the Peano network is a deterministic binomial multiplicative process having partition parameter equal to 1/4. This have hydrological implications as slight perturbations in the network length structure (topology remaining the same) determine large variations of the width function [*Veneziano et al*., 2000]. As also mentioned in section 1, the use of the Peano network has to be qualified by acknowledging that the topological characterization of real and Peano networks only provide a partial picture of relevant channel network features affecting hydrologic response and transport processes [*Rinaldo et al*., 1998].

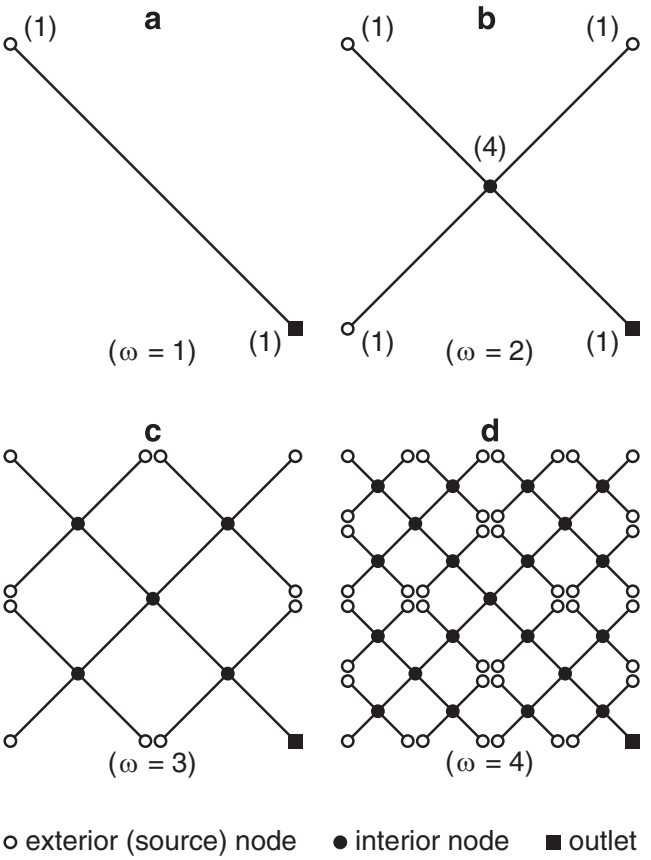

Figure 3. Construction of the Peano network having Horton-Strahler hierarchical order equal to four. The numbers of connections to interior and exterior nodes are reported, for instance, at the first and second steps reported in Figures 3a and 3b, respectively.

The Peano network of order ω can be constructed through an iterative procedure as sketched in Figure 3. Specifically, at the order $\omega = 1$ it is represented by a single segment stream, the initial generator segment, with only two exterior nodes (Figure 3a). The Peano network at the order $\omega = 2$ is obtained by crossing, at right angles and in the middle point, the initial generator segment with another segment stream, and then it is constituted by four segments and five nodes, four exterior nodes, and one internal node (Figure 3b). To obtain the Peano network at the order $\omega = 3$ we cross, at right angles and in the middle point, each segment of the Peano network at the order $\omega = 2$ with another segment stream so as to obtain a channel network formed by 16 segments, 12 exterior nodes, and 5 interior nodes (Figure 3c). This procedure can be iterated and the number of segments and junction nodes evaluated (Figure 3d for $\omega = 4$). Structural parameters of the Peano network can be calculated from recursive relationships as reported in Appendix A. In a Peano network, the junction degree of a node, k_n, is equal to 1 for the exterior (source) and outlet nodes, and it is equal to 4 in the interior nodes. Hence, *Horton*ian and Peano networks are topologically different at the local scale. At the arbitrary stage of generation Ω, and for a generic order ω ($\omega = 1, \ldots, \Omega$), it can be obtained from equation (2) that the average junction degree for the Peano network is

$$\langle k_n(\omega)\rangle = \frac{2}{1+\left(\frac{1}{4}\right)^{\omega-1}}. \tag{7}$$

In equation (7), the numbers of exterior and interior nodes are obtained through the equations (A7) and (A8), respectively. It is important to observe that equation (7) yields rational values of $\langle k_n(\omega)\rangle$ for $\omega \geq 2$ [*De Bartolo et al.*, 2009]. Relation (7) is the foundation for the analytical model of the average junction degrees displayed by *Horton*ian substructures in real channel networks as shown in the next section.

2.3. Analytical Model of the Average Junction Degree

In this section, we introduce an analytical model of the average junction degree $\langle k_n(\omega,\gamma)\rangle$ obtained by perturbing equation (7) as given by

$$\langle k_n(\omega,\gamma)\rangle = \frac{2}{1+\left(\frac{1}{2\gamma}\right)^{\omega-1}}, \tag{8}$$

The perturbation parameter $\gamma > 0$ is denoted as "uniformity factor." This model makes it possible to parameterize both real and theoretical networks. We note that the function (8) satisfies the initial condition (1) mentioned in section 2.1 for any $\gamma > 0$, and the asymptotic condition (2) mentioned in section 2.1 for any $\gamma > 1/2$. This means that there are no channel networks with $\gamma < 1/2$, whereas for $\gamma = 1/2$ we simply configure an unrealistic network composed of source node segments only. In addition, equation (8) assumes

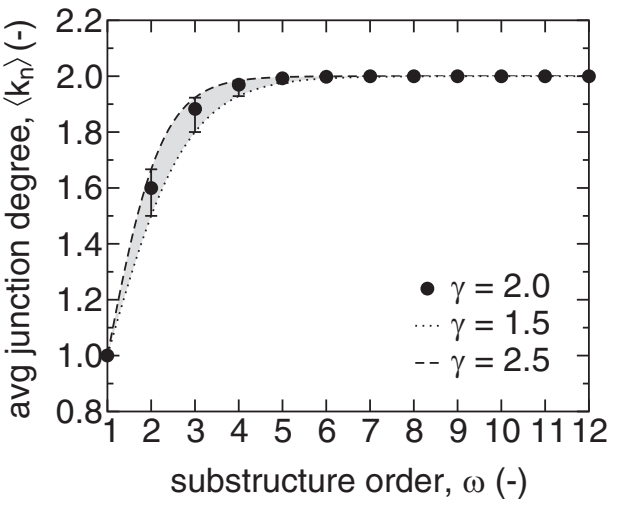

Figure 4. Sensitivity of the average junction degree $\langle k_n(\omega,\gamma)\rangle$ given by equation (8) to the perturbation parameter γ for Hortonian substructures having order ω ranging from 1 to 12. Solid circles refer to the case $\gamma = 2$ (Peano network). The bars indicate the variability obtained by varying γ from 1.5 (lower bound) to 2.5 (upper bound).

rational values when γ is a rational number as also implied by equation (4). As also noted in section 2.2, *Horton*ian and Peano networks are topologically different at the local scale. However, they may be topologically similar in global terms of average junction degrees $\langle k_n\rangle$ and uniformity factor γ. As shown in Figure 4, the average junction degree has little discriminatory power in the asymptotic range, namely for structures having orders ω greater than 4. However, the average junction degree is effective in discriminating network structures in the preasymptotic range, namely for structures having order ω less than or equal to 4, and this has a significant effect on the value of the uniformity factor, which is directly affected by the values of the average junction degree displayed by substructures in the preasymptotic range. In order to compare a generic *Horton*ian network with the Peano network of the same order Ω, the focus has to be put on the totality of substructures of these networks having order $\omega = 1, \ldots, \Omega$. For the Peano network, the average junction degree can be computed directly from equation (7). The perturbed equation (8) offers a suitable means for modeling real *Horton*ian networks, where the parameter γ is computed from a nonlinear regression over the average junction degrees of all *Horton*ian substructures. The uniformity factor γ is the means for capturing the discriminatory power displayed by the average junction degree in the preasymptotic range of Hortonian substructures.

Relation (8) provides a further development of the relationship found by *De Bartolo et al*. [2009] as it connects $\langle k_n(\omega,\gamma)\rangle$ and ω through the single parameter γ. The parameter γ provides a measure of dissimilarity (or topological similarity) between a real channel network and the Peano network. The case of the Peano network (equation (7)) can be recovered from equation (8) with $\gamma = 2$. For any real channel network the values of γ is obtained from a nonlinear regression of the relationship (8) on the data points $(\omega, \langle k_n(\omega)\rangle)$ with $(\omega = 1, \ldots, \Omega)$ computed on extracted Hortonian substructures. In fact, the perturbed equation (8) provides an analytical model of real channel networks as characterized by their Hortonian substructures.

The values of $\langle k_n\rangle$ provided by equation (8) display sensitivity to the variation of γ around 2 that vary with the order ω. In fact, according to the first-order Taylor series approximation, we can replace the equation (8) with

$$\langle k_n(\omega,\gamma+\delta\gamma)\rangle = \langle k_n(\omega,\gamma)\rangle + \frac{d}{d\gamma}\langle k_n(\omega,\gamma)\rangle\delta\gamma + \ldots, \tag{9}$$

where

$$\frac{d}{d\gamma}\langle k_n(\omega,\gamma)\rangle = \frac{2^{2-\omega}\left(\frac{1}{\gamma}\right)^{\omega}(\omega-1)}{\left[1+2^{\omega-1}\left(\frac{1}{\gamma}\right)^{\omega-1}\right]^2}. \tag{10}$$

On the basis of equation (10), it can be found that, for a neighborhood of $\gamma = 2$, the maximum variation of $\langle k_n(\omega,\gamma)\rangle$ occurs for $\omega = 2$. Gradually decreasing values of $d\langle k_n(\omega,\gamma)\rangle/d\gamma$ can be obtained for orders $\omega > 2$. In Figure 4 the values of $\langle k_n(\omega,\gamma)\rangle$ versus ω, with γ ranging from 1.5 to 2.5, are reported.

2.4. Drainage Density of Peano Grid and Channel Networks

The drainage density for a generic Peano grid network and for a Peano channel network is equal to

$$D = \frac{L_{\Omega}^{(T)}}{A} \tag{11}$$

and

$$D_C = \frac{L_{\Omega_C}^{(T)}}{A}, \tag{12}$$

where A represents the Peano basin area, while $L_{\Omega}^{(T)}$ and $L_{\Omega_C}^{(T)}$ are the total segment lengths of all orders in grid and channel networks, respectively. The analytical expressions of these total lengths are provided in Appendix B. Specifically, in equation (12) the total length, $L_{\Omega_C}^{(T)}$ depends on the threshold method used to extract the Peano channel network, as given by equations (B9) and (B13). It is important to observe that, in the case of Peano grid network, the limits of $h \to 0$ and $h \to \infty$ imply a divergence of measure, namely $D(h \to 0) = \infty$ and $D(h \to \infty) = 0$, respectively.

As detailed in Appendix B, the drainage density of the Peano network, generated as a grid or a channel network over a grid domain having size $2^n \times 2^n$ ($n = 1, 2, \ldots$), can be evaluated as the total length of channels of all orders ω (equations (B4), (B9), and (B13)) per unit area of the Peano basin ($2^n \times 2^n \times h^2$). In fact, as shown in Figure 5, the Peano grid network, and consequently the Peano channel network, can only be constructed on square grid domains having size $2^n \times 2^n$. As suggested by *Tucker et al*. [2001], maps of drainage density D can be computed from digital terrain data as $D = 1/(2\bar{L})$, where $\bar{L}$ is the mean hillslope-to-channel length along drainage paths. Averaging length-to-channel over an appropriate spatial scale makes it possible to derive continuous maps of D and its spatial variations. This method is consistent with the standard definition of drainage density, defined by *Horton* [1932] as the total length of channels per unit area, which is directly used to compute the drainage density at the drainage basin scale in the present study.

In the case of Peano grid network, the maximum order Ω is related to the exponent n in the grid domain size through the relation

$$\Omega = n + 1. \tag{13}$$

Therefore, Ω does not depend on the grid cell size, h, but only on the grid domain size. In the case of a generic Peano channel network, the first parameter that has to be defined is the threshold quantity for channel initiation (Figure 5). Only the drainage area A and Horton-Strahler order ω^* can be used as threshold quantities, because the local slope S used in the slope-area quantity AS^2 in undefined in Peano grid networks, which grows on a 2-D plane. The threshold value A_t is linked, in the case of the Peano grid network, to the grid cell size h through the equation

$$A_t = 4^m h^2, \tag{14}$$

where the exponent m is a fixed integer ranging between 1 and Ω. If m is fixed, then the maximum order Ω_C of the Peano channel network is obtained by the equation

$$\Omega_C = \Omega - m. \tag{15}$$

For a fixed threshold value ω_t^*, the maximum order Ω_C of the Peano channel network is given by

$$\Omega_C = \Omega - \omega_t^*. \tag{16}$$

3. Numerical Experiments

3.1. Hortonian Substructures Analysis

To investigate the average junction degree to the order ω, we analyzed grid and channel networks extracted from grid DEMs by using the D8-LTD method [*Orlandini et al*., 2003, 2014]. The grid networks are determined by connecting all grid cell centers along the determined surface slope paths [*Orlandini and Moretti*, 2009]. As also mentioned in section 1, the channel networks are obtained from grid networks by filtering the cells that display a value of the drainage area A, of the slope-area function AS^2, or of the Strahler order ω^* less than fixed threshold values A_t, $(AS^2)_t$, and ω_t^*, respectively. This procedure was repeated for different resolutions h, from 1 to 50 m, obtained by coarse graining the original 1 m DEM. Eight drainage basins, namely the RC1, RC2, RC3, TC1, TC2, TC3, GM1, and AP1, were analyzed. The locations of the real networks considered in the present study are reported in Figure 6. The RC1, RC2, and RC3 are subbasins of the Rio Cordon drainage basin and are located in the Italian Alps, Italy. The TC1, TC2, and TC3 are subbasins of the Crostolo River drainage basin and are located in Italian Apennines. The GM1 is a drainage basin of the Gabilan Mesa region located in California, USA. The AP1 is a drainage basin of Allegheny Plateau region

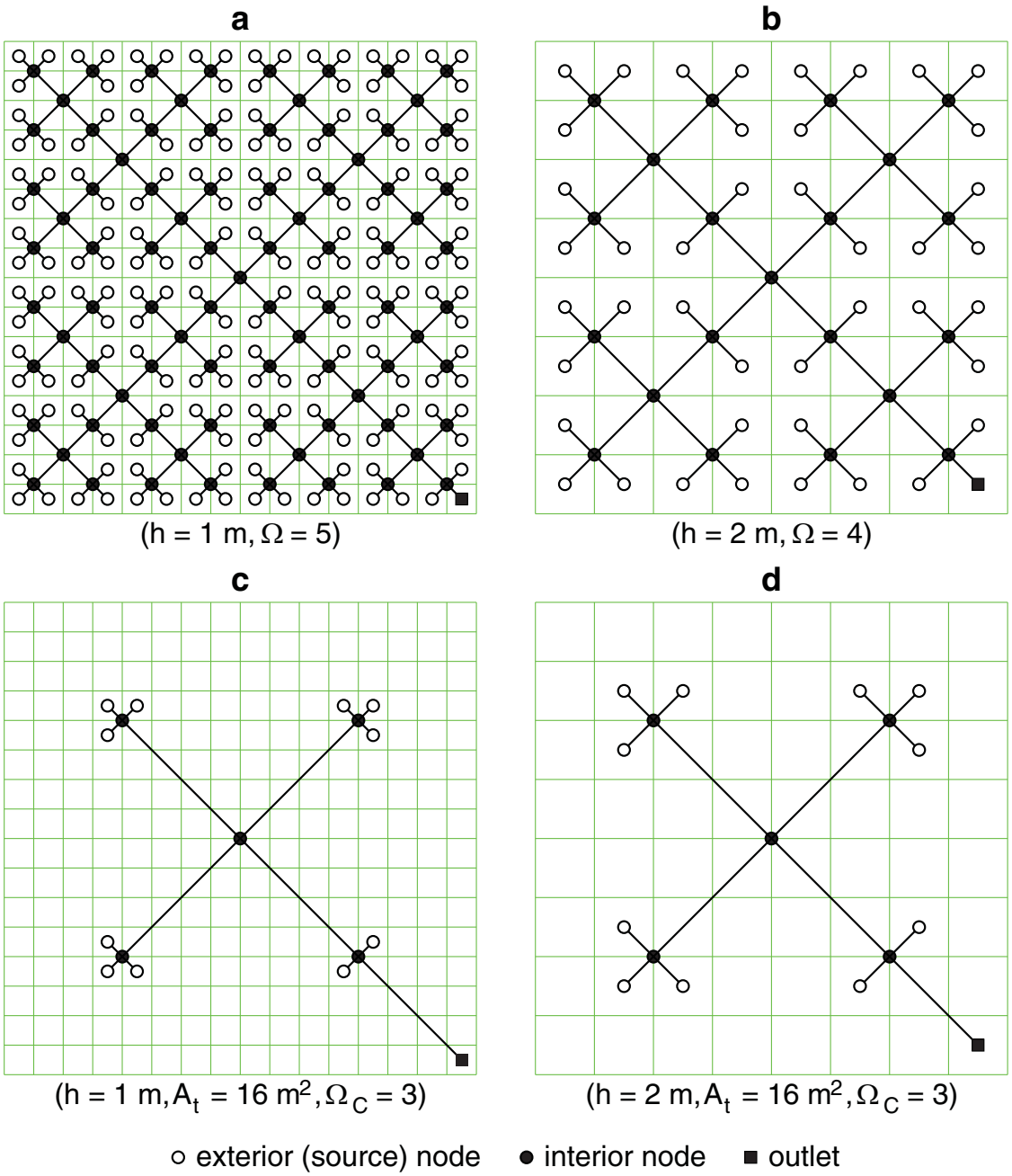

Figure 5. Peano grid (Figures 5a and 5b) and channel (Figures 5c and 5d) networks generated in grids with $2^4 \times 2^4$ cells and resolution $h = 1$ m (Figures 5a and 5c), or in grids with $2^3 \times 2^3$ cells and resolution $h = 2$ m (Figures 5b and 5d). Peano channel networks were obtained by setting the threshold area A_t equal to 16 m^2.

located in Pennsylvania, USA. In this last case, the extraction procedure was repeated for the resolutions obtained by coarse graining the original 2 m DEM. The areas of RC1, RC2, RC3, TC1, and TC2 subbasins are equal to 0.455, 0.081, 0.708, 0.152, and 0.121 km^2, respectively, whereas the areas of GM1, AP1, and TC3 subbasins are greater and are equal to 1.81, 3.91, and 87.3 km^2, respectively.

The channels observed in the RC1, RC2, and RC3 drainage basins can be classified as colluvial, bedrock, and alluvial channels [*Orlandini et al.*, 2011]. The colluvial incisions are small headwater channels, exhibiting a weak or ephemeral transport capacity [*Montgomery and Buffington*, 1997]. The alluvial channel network is dominated by erosional and depositional processes controlled mainly by local slope changes, where the sediment forming the channel bed can be transported and organized during

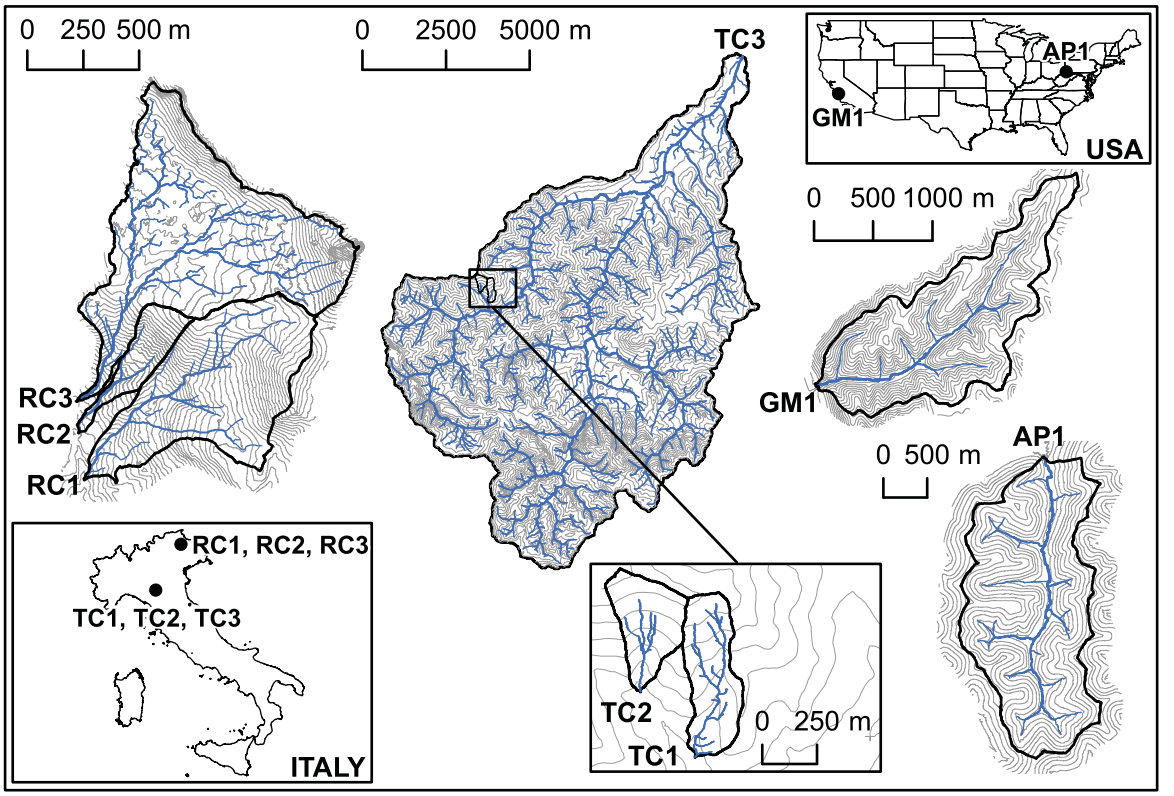

Figure 6. Location and representation of the real networks considered in the present study.

floods. In the drainage basins TC1, TC2, and TC3, both colluvial and alluvial channels were surveyed, with dominance of colluvial channels in TC1 and TC2, and alluvial channel in TC3. In the drainage basins GM1 and AP1, smooth, soil-mantled slopes surround partially vegetated channels incised into colluvium [*Perron et al.*, 2012]. The lidar surveys were all carried out, during snow-free conditions. Lidar data and high-resolution aerial photographs were acquired from a helicopter or an airplane. In the RC1, RC2, and RC3, the survey design point density was specified to be greater than 5 points/m^2, recording up to four returns, including first and last. The mean absolute vertical accuracy, evaluated by a direct comparison between lidar and ground DGPS elevation points, was estimated to be less than 0.3 m [*Pirotti and Tarolli*, 2010]. The lidar data for the TC1, TC2, TC3, GM1, and AP1 drainage basins display a similar accuracy. The lidar bare ground data set was used to generate accurate 1 or 2 m DEMs. The natural neighbor technique was used for this operation [*Sibson*, 1981].

The threshold parameters (A_t, $(AS^2)_t$, and ω_t^*) were evaluated from accurate observations of channel heads, both of the subbasins of the Cordon River and of the Crostolo River (TC1 and TC2). A total of 52 channel heads were mapped using field survey through a differential global positioning system (DGPS) system. The threshold conditions were defined from an overlap of the channel heads observed on the grid networks extracted by using the D8-LTD method. The channel networks of the TC3 were obtained, for the different grid cell sizes, by imposing as threshold values the averages of the threshold values obtained in the TC1 and TC2 subbasins. This assumption was essentially made for two reasons. First, the large extension of the TC3 implies a prohibitive cost of extensive field surveys for the localization of the channel heads. Second, lithology, morphology, and land use was found to be reasonably homogeneous across the entire subbasin. The channel networks of the GM1 and AP1 drainage basins were determined by searching the best agreement between the channel networks extracted from digital elevation models at the finest available resolutions and the channel networks revealed visually in the digital elevation model hillshades. Grid cell sizes of 1 and 2 m were used for the GM1 and AP1, respectively. At these fine resolutions, the hillshades of the GM1 and AP1 drainage basins were found to highlight clearly the morphology of channels and, specifically, the

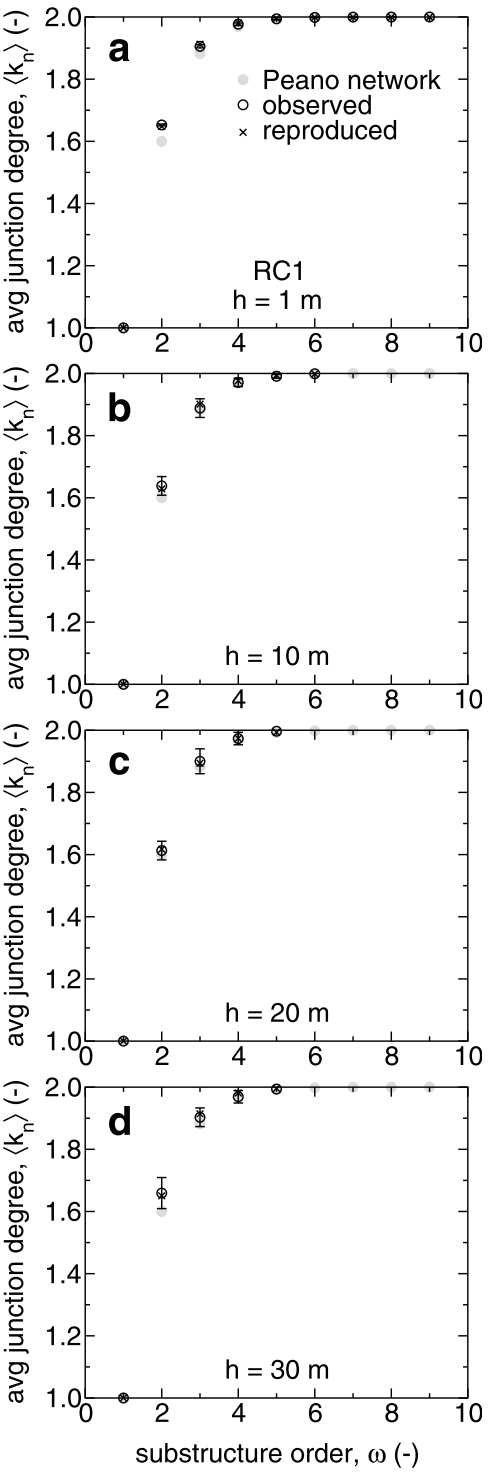

Figure 7. Comparison between values of $\langle k_n(\omega)\rangle$ and $\langle k\tilde{\gamma}(\omega)\rangle$ obtained in the cases of the RC1 grid networks at different resolutions *h*. The $\tilde{\gamma}$ parameter is obtained from a nonlinear regression based on equation (8) over observed values of $\langle k_n(\omega)\rangle$.

heads of these channels. The values of the threshold quantities for channel initiation were varied in the channel network extraction program and the best values were simply obtained by applying a trial-and-error procedure.

A total of 1008 real channel network structures were analyzed. These structures were hierarchized through the Horton-Strahler ordering system and compared with the Peano network. The outlet orders obtained by this classification procedure are between 3 and 12 for the grid networks, and between 2 and 10 for the channel networks. The first step was to evaluate the number of network substructures obtained from the hierarchization procedure. This number, for each subbasin structure and for all spatial resolutions analyzed, is a function of the hierarchical order ω, and presents a decreasing exponential trend whose maximum values appear to be in correspondence to the network magnitude, that is the number of exterior nodes in the network [*Horton*, 1945; *Giusti and Schneider*, 1965; *Shreve*, 1966a,b; *Peckham*, 1995b]. Regarding the grid networks, it was observed that the substructures *n*(2, *i*) have a decreasing trend of occurrences for all network subbasin structures analyzed (2). In contrast, for the network substructures *n*(3, *i*), we found a unimodal trend limited to a narrow range, between 5 and 10, of *i* source nodes for all network subbasin structures examined (Figure 2). Specifically these trends are univocal in correspondence to the maximum spatial resolution, 1 m, and anyway well-defined up to the spatial resolution of about 7 m for the RC1, RC2, RC3, TC1, and TC2 network subbasin structures, and for all the resolutions in the case of TC3, GM1, and AP1 network subbasin structures. In the case of the channel networks of the RC1, RC2, RC3, TC1, and TC2, this behavior presents a unpredictable trend for both $\omega = 2$ and $\omega = 3$. It was observed that the number of network substructures, to the second hierarchical order with *i* source nodes, decreases as the number of source nodes increases, as in the case for grid networks. Similar behaviors were observed for the TC3, GM1, and AP1 channel networks, owing to the high number of network substructures obtained for both $\omega = 2$ and $\omega = 3$. These results agree with the values found by *Giusti and Schneider* [1965] and *Shreve* [1966a,b] in the context of the distribution of branches in Hortonian river networks.

3.2. Estimation of the Average Junction Degree

Once all substructures of order ω with *i* source nodes are identified, the average junction degree $\langle k_n(\omega)\rangle$ was calculated directly through the equation (4), for all the hierarchical orders ω. The case of the RC1 is reported, for instance, in Figure 7. Error bars were estimated by computing the error ε in the counting of Hortonian substructures with *i* source nodes as given by

$$\epsilon = \frac{\sum_{i=2^{\omega-1}}^{2^{\omega-1}+L-1} \left| \frac{1}{i} \sum_{j=2^{\omega-1}}^{2^{\omega-1}+L-1} n(\omega,j) - \sum_{j=2^{\omega-1}}^{2^{\omega-1}+L-1} \frac{n(\omega,j)}{j} \right| \sqrt{n(\omega,i)}}{\left(\sum_{i=2^{\omega-1}}^{2^{\omega-1}+L-1} n(\omega,i) \right)^2}. \quad (17)$$

This error was evaluated by means of a Poisson distribution of the $n(\omega,i)$ counting, with a corresponding error $\sqrt{n(\omega,i)}$ and then propagated through the usual techniques of asymptotic expansion [*Taylor*, 1997]. Finally, the relative differences between the values of $\langle k_n(\omega) \rangle$ obtained for Hortonian substructures and those obtained for the corresponding Peano networks were calculated. It was obtained from the analysis of grid networks, for all analyzed grid cell sizes, that the numerical values of the average junction degree corresponding to $\omega = 2$, are in the range between 1.553 and 1.756 for the RC1, RC2, RC3, TC1, and TC2 network subbasin structures, with average equal to 1.625, and between 1.616 and 1.665 for the TC3, GM1, and AP1 subbasin structures. Instead, in the case $\omega = 3$, they are between 1.878 and 1.968 for the RC1, RC2, RC3, TC1, and TC2 network subbasin structures, with average value equal to 1.901, and between 1.858 and 1.930 for the TC3, GM1, and AP1 network subbasin structures.

The descriptor $\langle k_n(\omega) \rangle$ assumes, for all network structures analyzed, values greater than 1.955 for the remaining hierarchical orders and tends asymptotically to 2 in correspondence to hierarchical closure orders of the entire networks extracted. Regarding the values of the error bars and of the relative differences compared to Peano, the eight structures of the grid networks showed values, for all ω orders, ranging between 10^{-7} and 10^{-2}, and between 10^{-7} and 10^{-1}, respectively. For the channel networks extracted by using the three thresholds (A, AS^2, and ω^*), the numerical values of the $\langle k_n(\omega) \rangle$, relatively to $\omega = 2$, are between 1.500 and 1.875 for the RC1, RC2, RC3, TC1, and TC2 network subbasin structures, with average equal to 1.648, and between 1.500 and 1.888, for the TC3, GM1, and AP1 network subbasin structures. For the RC1, RC2, RC3, TC1, and TC2 substructures at the $\omega = 3$, instead, the values range between 1.750 and 1.974, with average equal to 1.886. In the case of TC3, GM1, and AP1 channel networks, these values range between 1.795 and 1.976. For the remaining hierarchical orders and to the hierarchical closure, the descriptor assumes values greater than 1.941 and tends asymptotically to 2. The values of the error bars and of the relative differences with respect to the Peano networks, the eight structures of the channel networks showed values, for all ω orders, ranging between 10^{-6} and 10^{-1}.

Table 1. Values of the Uniformity Factor γ for the Crostolo Channel Network

h (m)[a]	$\tilde{\gamma}$[a]	SE[a]	EV ($\times 10^{-5}$)[a]
1	2.086	0.004	0.054
2	2.047	0.018	1.200
3	2.058	0.014	0.730
4	2.065	0.007	0.170
5	2.043	0.011	0.430
6	2.058	0.008	0.230
7	2.060	0.008	0.250
8	2.056	0.007	0.190
9	2.088	0.008	0.200
10	2.110	0.006	0.130
11	2.092	0.004	0.061
12	2.103	0.005	0.083
13	2.098	0.006	0.120
14	2.116	0.011	0.420
15	2.138	0.005	0.063
16	2.114	0.006	0.130
17	2.114	0.023	1.700
18	2.086	0.008	0.230
19	2.090	0.004	0.041
20	2.082	0.004	0.057
21	2.086	0.007	0.180
22	2.079	0.009	0.270
23	2.081	0.007	0.180
24	2.101	0.012	0.510
25	2.144	0.023	1.500
26	2.128	0.007	0.150
27	2.120	0.008	0.210
28	2.103	0.017	0.890
29	2.098	0.007	0.160
30	2.126	0.010	0.090
35	2.124	0.008	0.190
40	2.128	0.014	0.640
45	2.149	0.009	0.260
50	2.173	0.019	0.110

[a]h: grid cell size; $\tilde{\gamma}$: estimate asymptotic value for the uniformity factor γ; SE: standard error; EV: estimated variance.

3.3. Estimation of the Uniformity Factor

The estimated values of the uniformity factor γ, namely $\tilde{\gamma}$ in the numerical cases, obtained from the perturbed model (8), for each set of extracted Hortonian substructure of order ω ($\omega = 1, \ldots, \Omega$), were computed by using a nonlinear regression on the computed data points $(\omega, \langle k_n(\omega) \rangle)$. This procedure was based on a nonlinear least squares "gradient" method algorithm included in Mathematica (Version 9.0). In Table 1, the results regarding the TC3 channel network generated by using a threshold on ω^* are reported as an example. Specifically, estimated asymptotic value (EAV), the standard error (SE), and the estimated variance (EV), are reported. Similar values were obtained for all the other drainage basins. In Figure 7, the average junction degrees $\langle k_n(\omega) \rangle$ calculated for the

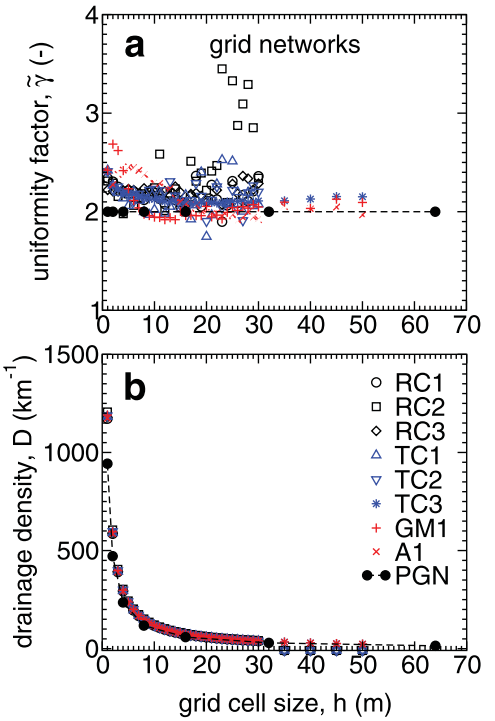

Figure 8. Uniformity factor $\tilde{\gamma}$ and drainage density D for the real and Peano grid networks analyzed.

RC1 grid network substructures (equation (4)) have been reported along with the related error bars (equation (17), the estimated average junction degrees $\langle k\tilde{\gamma}(\omega)\rangle$ (equation (8)), and the values of the calculated for the Peano deterministic network (equation (7)). For each examined case, the value of $\langle k\tilde{\gamma}(\omega)\rangle$ lies in the error bars of the average junction degree $\langle k_n(\omega)\rangle$ calculated from equation (4).

As shown in Figures 8 and 9, the parameter $\tilde{\gamma}$ was found to vary with the grid cell size h. For the grid and channel networks, the trends of $\tilde{\gamma}$ evaluated for different grid cell sizes are reported in Figures 8a and 9a–9c. More specifically, for the grid networks of the RC1, RC2, RC3, TC1, and TC2 drainage basins, $\tilde{\gamma}$ decreases as grid cell size decreased, on average for h lying between 1 and 3 m, and is essentially constant for grid cell sizes ranging between 3 and 10–15 m (Figure 8a). In contrast, the trend of TC3 network subbasin is different, which showed, a decreasing trend of $\tilde{\gamma}$, with an asymptotic behavior for grid cell sizes lying between 10 and 30 m (Figure 8a). Instead, the values of $\tilde{\gamma}$ observed for grid cell sizes lying between 30 and 50 m tend to increase and to depart from the values obtained for the Peano network (Figure 8a). A similar behavior was observed in the GM1 substructures, where the values of $\tilde{\gamma}$ tend to decrease until grid cell size h are about equal to 10 m and to increase for grid cell sizes in the range between 20 and 25 m (Figure 8a). In the case of AP1 substructures, the values of $\tilde{\gamma}$ tend to increase for grid cell sizes ranging between 2 and 5 m, whereas the values of $\tilde{\gamma}$ decrease until the grid cell size 20 m is reached. Finally, these values are constant for grid cell sizes ranging between 20 and 30 m and tend to increase for grid cell sizes ranging between 30 and 50 m (Figure 8a).

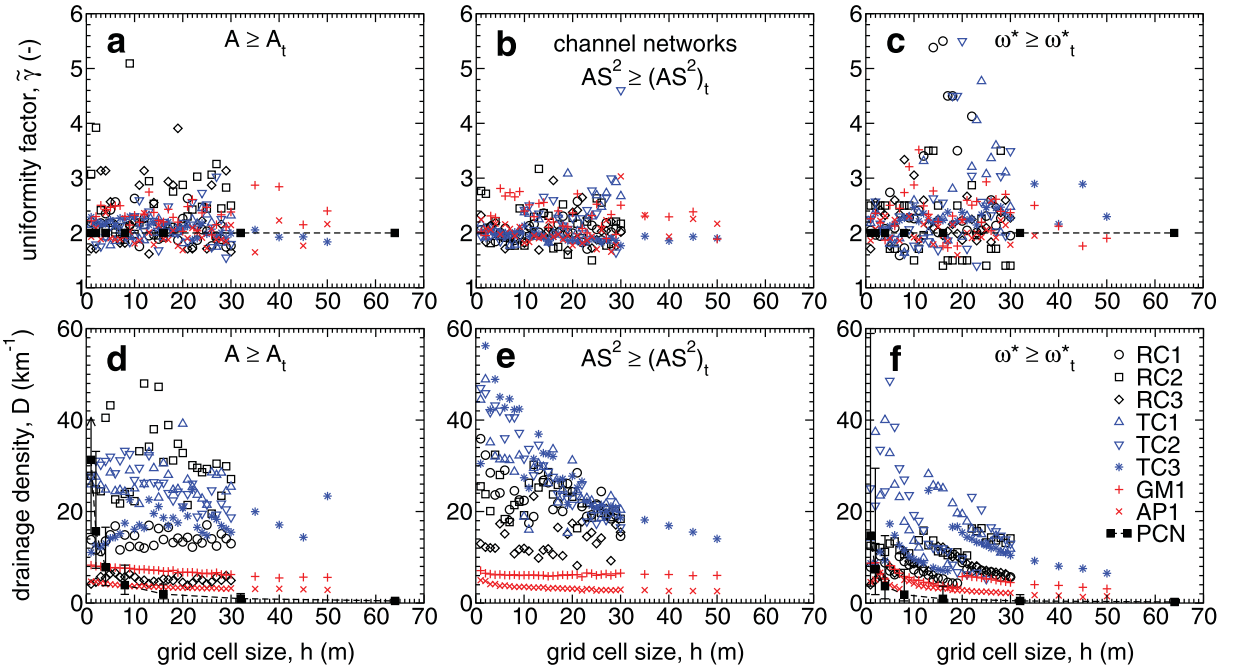

Figure 9. Uniformity factor $\tilde{\gamma}$ and drainage density D for the real and Peano channel networks analyzed, as obtained from the A, AS^2 and ω^* threshold methods.

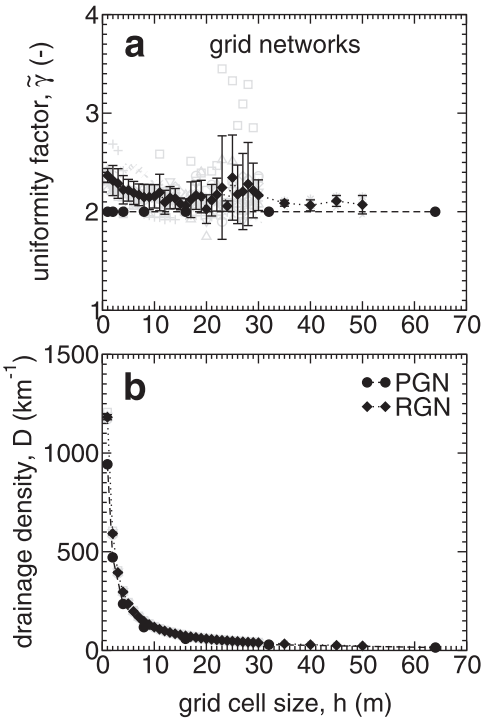

Figure 10. Average uniformity factor $\tilde{\gamma}$ and average drainage density D for the real and Peano grid networks analyzed. Standard deviations of the averaged values are used to calculate the lower and upper limits of uncertainty bars.

Generally, in the channel networks extracted by applying the three methods for channel initiation mentioned above, the $\tilde{\gamma}$ trend appears to be constant until the grid cell size of about 1 to 10–15 m is reached, for the RC1, RC2, TC1, and TC2 networks (Figures 9a–9c). Differently, the RC3 network assumes a fluctuating trend in response to changes in grid cell size. The case of the TC3 subbasin shows a constant trend of the uniformity factor $\tilde{\gamma}$ in the first 8–10 m, regardless threshold method used. The GM1 and AP1, for grid cell sizes less than 10 m, showed the same trend of TC3. The trend of $\tilde{\gamma}$ depends in any case on the threshold method used (Figures 9a–9c).

As shown in Figure 10, the average values of the uniformity factor $\tilde{\gamma}$ computed over all river structures analyzed show a more defined trend. Specifically, in Figure 10a it is shown the behavior of $\tilde{\gamma}$ in the case of grid networks. In this case, the uniformity factor assumes a decreasing trend for grid cell sizes lying in the range between 1 and 10 m, and fluctuating trends until to the grid cell size of 30 m is reached. The values of $\tilde{\gamma}$ obtained for grid cell sizes ranging between 30 and 50 m display a constant trend. Regarding the channel networks, instead, as reported in Figures 11a–11c, the average values of the uniformity factor $\tilde{\gamma}$ show for the thresholds $(AS^2)_t$ and ω_t^*, a constant trend for grid cell sizes ranging from 1 to 8–10 m and a fluctuating trend until the grid cell size of 50 m is reached. These fluctuations are clearer when the threshold ω_t^* is used (Figure 11c). The constant trend behavior is better defined with respect to the case in which the threshold $(AS^2)_t$ is used (Figure 11b). When the threshold A_t is used, this behavior display less variability for grid cell sizes ranging from 1 to 30 m.

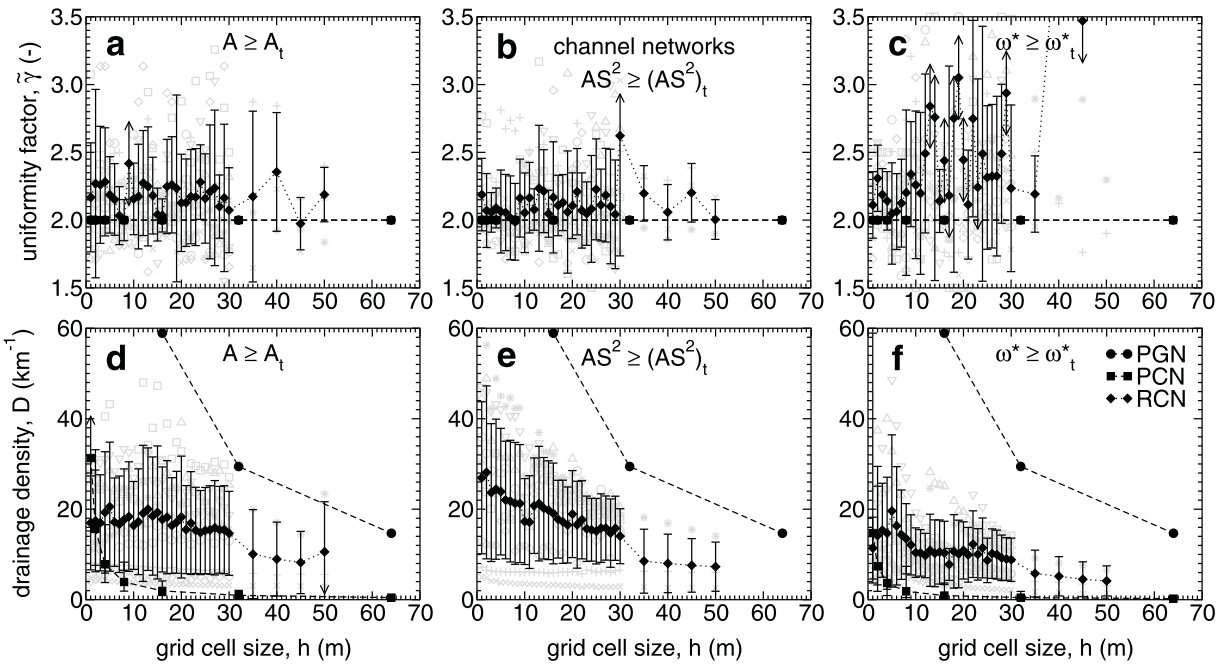

Figure 11. Average uniformity factor $\tilde{\gamma}$ and average drainage density D for the real and Peano channel networks analyzed, as obtained from the A, AS^2 and ω^* threshold methods. Standard deviations of the averaged values are used to calculate the lower and upper limits of uncertainty bars.

3.4. Estimation of the Drainage Density

The coarse graining analysis reported above has focused on the variation of the parameter $\tilde{\gamma}$ with grid cell size in high-resolution DEMs for both Hortonian and Peano networks. The relation between grid, channel, and Peano networks can be further investigated by analyzing the variation with grid cell size of the drainage density, D, which is a measure of the length of stream channel per unit area of drainage basin. Numerically, this geomorphological feature is calculated by using the relationships

$$D=\frac{L_T}{A_\Omega}=\sum_{\omega=1}^{\Omega}\sum_{i=1}^{N_\omega}\frac{L_{\omega i}}{A_\Omega}=\sum_{\omega=1}^{\Omega}\frac{N_\omega \bar{L}_\omega}{A_\Omega}, \tag{18}$$

where L_T is the total length of the channels of all orders within river basin, A_Ω is the total area of the basin to greater order Ω, while N_Ω and $\bar{L}_\omega$ are the average number and length of the streams of order ω, respectively [*Bras*, 1990]. In the Peano networks, the drainage densities can be calculated by using the relationships (11), (B11), and (B12), for Peano grid and channel networks and depending on the considered threshold condition for channel initiation. Peano networks are generated on a square drainage basin having extension of about 67 km^2 (a comparable extension to the largest real drainage basin considered) for grid cell sizes of 1, 2, 8, 16, 32, and 64 m. These quantities are compatible with the requirement reported in section 2.4 that the grid domain size is $2^n \times 2^n$ with $n=7,\ldots,13$.

It is observed that the drainage density D decreases as the grid cell size h increases, for both channel and Peano networks. This behavior is clearly shown in Figure 8b. It is important to observe that the drainage density in the Peano grid case overlaps the curves obtained from analysis of D for the observed natural networks. The values of drainage density, by construction of the same Peano network, are lower than the values obtained for the natural networks analyzed, for the small values of h. This result is, however, consistent with the limit $D(h \to 0)=\infty$. The drainage density behavior shown in this study was observed in many studies reported in the literature [e.g., *Tarboton et al*., 1988, 1991], *Bras* [1990], *Helmlinger et al*. [1993], *Dodds and Rothman* [1999], *Yang et al*. [2001]. In the case of Crostolo channel network TC3, the values of drainage density preserve an affine behavior with the uniformity factor for grid cell sizes ranging from 1 to 25 m (Figure 8a and 8b). In addition, the average values of the drainage density D show on average for all river structures the same behavior observed for each channel network analyzed. These values, in fact, are almost the same for all natural channel network and for all spatial resolutions (Figure 10b).

Furthermore, the drainage density behavior is found to depend on the thresholds on A, AS^2, and ω^*. Also for this channel-scale representation, the results agree with those observed in *Bras* [1990], *Helmlinger et al*. [1993], and *Dodds and Rothman* [1999]. These researchers have shown that there is an effect of the parameter choice on the morphometric properties of the river basin. For example, in addition to the drainage density, also the scaling properties of channel networks are affected by the spatial scale selected. In particular, according to *Dodds and Rothman* [1999] and *Tucker et al*. [2001], the uniform drainage density may also be interpreted as the observation that the average distance between channels is roughly constant across a landscape. This is due to the fact that there is a finite limit to the channelization of a landscape determined by a combination of soil properties and climate. Furthermore, the average distance between streams being roughly constant implies that, on average, tributaries are spaced evenly along a stream. Implicit in this assumption is that the channel network has reached its maximum extension into a landscape [*Dodds and Rothman*, 1999]. These characteristics, by virtue of the topological properties of river networks [*De Bartolo et al*., 2009], are preserved also for junction nodes and then a proper analysis of the average junction degree is congruent.

At channel scale, it is possible to observe that the channel river networks extracted by using a threshold on the drainage area A show a less variable trend in the first 10 m than those observed for the channel networks extracted by using thresholds on ω^* and AS^2, which show some peaks at high resolutions (Figures 10d–10f). In the case of the Crostolo channel network TC3 extracted by using a threshold on A, the affinity behavior with the parameter γ is more evident in the previous scaling range (Figures 9a and 9d). Therefore, in the context of coarse graining and when the threshold on A is used, the two parameters appear to be affine, showing a same trend with grid cell size for the fine-resolution river structures. Also in this case, as a result, it is observed that this uniformity factor γ appears to be confined in a precise scaling range of cell measures restricted between 1 and 10 m. In fact, according to *Dodds and Rothman* [1999], this metric

homogeneity/uniformity is representative since some fundamental features of these structures were removed by coarse graining the small grid cell sizes. In terms of topography, this behavior confirms, as the results previously obtained, the existence of an invariant scaling range that is indicative of a correct extraction criterion of channel network for both grid and channel scale in addition to the equivalence between the drainage density, D, and the uniformity factor γ.

Furthermore, at the channel scale, the drainage density was calculated on the Peano channel network obtained by filtering the segments of the Peano grid network and by using thresholds on the drainage area A and on the Horton-Strahler order ω^*. The threshold values used, in terms of A_t and ω_t^*, are in the ranges between 64 and 4096 m^2, and between 2 and 5, respectively. Analyzing the plots in Figures 11d and 11f, for all natural river networks, it is possible to observe that the drainage density remains on average almost constant. It is also observed that values of D are greater than those obtained for the Peano channel network, with the exception for small grid cell sizes. Finally, the threshold on A has shown a higher level of constancy and stable values of D for variable grid cell size.

4. Discussion

The relation between grid, channel, and Peano networks was investigated in the present study by analyzing the networks extracted from high-resolution digital elevation models data based on lidar surveys of eight real drainage basins located in four different geographical areas (section 3, Figure 6). The concept of average junction degree $\langle k_n \rangle$ and the related concept of uniformity factor γ used in the present study (section 2) were shown to have discriminatory power for the topological characterization of theoretical and real networks in the preasymptotic range of Strahler orders ω, that is for moderate values of ω ranging between 2 and 4 (Figure 4). This is relevant to the characterization of all channel networks because Hortonian substructures with ω equal to 2, 3, and 4 are numerous in real drainage networks (Figure 2). However, since $\langle k_n \rangle$ and γ are partial topological descriptors of channel networks, the results reported in the present study can only be used to evaluate topological similarity or, if the evaluation is made a broader sense, dissimilarity between considered networks (Figures 7–11). The topological analysis based on $\langle k_n \rangle$ and γ reported in the present study is complemented, therefore, with the investigation of the drainage density D, which is one of the most relevant morphometric properties of channel networks in drainage basin hydrology (Figures 8–11).

Grid networks extracted from real topographic data display mostly values of γ greater than 2, which is the value associated to large Peano networks (Figures 8 and 9). On the basis of the analytical model (7) relating $\langle k_n \rangle$ and γ and of the sensitivity of $\langle k_n \rangle$ to γ illustrated in Figure 4, it can be inferred that Hortonian grid networks with $\gamma > 2$ display generally greater values of $\langle k_n \rangle$ in the preasymptotic range and thus a smaller fraction of exterior (source) nodes than Peano grid networks (section 4, Figure 8a). In fact, as noted in section 2.1, in Hortonian networks the junction degree k_n is equal to 1 for the exterior (source) and outlet nodes and it is normally equal to 3 for the interior nodes, being $k_n > 3$ observed only when fractures or junction faults occurs, whereas, as noted in section 2.2, in Peano networks k_n is equal to 1 for the exterior (source) and outlet nodes and it is equal to 4 in the interior nodes. Hence, given that k_n in interior nodes is generally smaller in Hortonian networks than in Peano networks, an average junction degrees $\langle k_n \rangle$ greater than 2 (the value associated to Peano networks) indicate a smaller fraction of exterior nodes than in Peano networks. The average values of γ displayed by real grid networks show a defined trend only for small values of the grid cell size h, with differences with respect to the value 2 of the Peano grid network that increases as h decreases (Figure 10a). This is likely to be connected to an increase of the degree of branching displayed by grid networks and well captured by the D8-LTD flow direction method [*Orlandini et al.*, 2003].

All the grid networks examined display the same trend of D with h (Figures 8b and 9b). This trend is clearly connected to the control on D of the representation of drainage paths at the elemental cell scale, consistently with *Tucker et al.*'s [2001] definition of drainage density mentioned also in section 2.4. In fact, the values of drainage density D reported in Figures 8b and 9b are explained by the relation $D = 1/(2\bar{L})$ with mean hillslope-to-channel length $\bar{L} \sim h/2$, and support therefore the morphometric equivalence between *Tucker et al.*'s [2001] relation and the original definition of drainage density given by *Horton* [1932] and used in the present study (section 3.4, equation (18)). The observed increase of D (from about 0.02 to 1000 km^{-1}) as h decreases (from 50 to 1 m, respectively) suggests that caution must be exercised when representing surface flow propagation along hillslope systems in detailed distributed hydrologic models [e.g., *Camporese et al.*,

2010]. The strong variability of D needs to be controlled in order to make surface flow and transport processes along hillslope systems independent from the selection of the structural parameter h.

Channel networks extracted from real topographic data by using thresholds for channel initiation on drainage area A, area-slope function AS^2, and Strahler order ω^* display both values $\gamma > 2$ and $\gamma < 2$, revealing that these channel networks do not necessarily display smaller fractions, respectively, of exterior nodes with respect to the corresponding Peano channel networks (Figure 9). An impact on the fraction of exterior nodes and related values of $\langle k_n \rangle$ and γ is also exercised by the selection of the threshold for channel initiation (Figures 9 and 11). The use of A and AS^2 yields a more robust scale invariance of average values of γ with h than the use of ω^* (Figures 9a–9c, 11a–11c). For any selected threshold for channel initiation, the obtained values of γ display significant fluctuations and large uncertainty bars, suggesting that the interrelationship between the characteristic scales of variability of land surface topographies and h may play a role.

The values of D displayed by real channel networks are found to vary significantly across different geographical areas (Figures 9d–9f). These values of D are mostly bounded between the corresponding values of Peano channel networks (lower bounds) and of Peano grid networks (upper bounds) as shown in Figures 11d–11f. The average values of D over the real drainage basins display well-defined trends with h, indicating that D assumes the same value as the Peano channel network for small values of h around 1–2 m, and the same value as the Peano grid network for large values of h around 50 m or more (Figure 11d–11f). This may explain, at least in part, the validity of previous applications of the Peano network to drainage basins represented by standard DEMs (i.e., not based on lidar surveys) with grid cell sizes h on the order of 50 m or more [*Marani et al.*, 1991; *Flammini and Colaiori*, 1996; *Troutman and Over*, 2001; *Veitzer and Gupta*, 2001; *Tay et al.*, 2006]. The results reported in Figures 9d–9f and 11d–11f indicates that more robust estimates of D with varying h are obtained by using the threshold for channel initiation on A in preference to AS^2 and ω^*. Even by changing the threshold values of AS^2 and ω^* with h as suggested in *Orlandini et al.* [2011], the values of D obtained by using these two thresholds are found to increase as h decreases, an evidence that needs to be investigated in future morphometric studies and to be acknowledged in distributed catchment modeling.

5. Conclusions

The ability of the average junction degree $\langle k_n \rangle$ and of the uniformity factor γ to relate grid, channel, and Peano networks was investigated in high-resolution digital elevation models over different grid cell sizes h and thresholds for channel initiation (Figures 6–11). Grid networks extracted from real topographic data display mostly values of γ greater than the value 2 of the Peano grid network (Figures 8 and 9), indicating greater values of $\langle k_n \rangle$ in the preasymptotic range of Strahler orders and thus smaller fractions of exterior (source) nodes than Peano grid networks (Figure 8a). The average values of γ displayed by real grid networks show a defined trend only for small values of h, with differences from the value 2 that slightly increases as h decreases (Figure 10a). All the grid networks examined display the same trend of drainage density D with h, an occurrence that can be explained by *Tucker et al.*'s [2001] relation $D = 1/(2\bar{L})$ with mean hillslope-to-channel length $\bar{L} \sim h/2$ (Figures 8b and 10b).

Channel networks extracted from real topographic data by using thresholds for channel initiation on drainage area A, area-slope function AS^2, and Strahler order ω^* display both values $\gamma > 2$ and $\gamma < 2$, revealing that these channel networks do not necessarily display smaller fractions of exterior nodes with respect to the corresponding Peano channel networks (Figures 9a–9c, 11a–11c). The values of D displayed by real channel networks are found to vary significantly across different geographical areas (Figures 9d–9f). The average values of D over the real drainage basins display, however, well-defined trends with h, indicating that D assumes the same value as the Peano channel network for small values of h around 1–2 m, and the same value as the Peano grid network for large values of h around 50 m or more (Figure 11d–11f).

The results obtained indicate that the topological relation between real and Peano networks may not vary over a wide range of grid cell sizes and threshold conditions for channel initiation. Real and Peano networks are however found to be morphometrically equivalent in terms of drainage density only for specific grid cell sizes, which may depend on the selected threshold for channel initiation. Future research is therefore

suggested on morphometric relations between grid, channel, Peano networks in high-resolution digital elevation models, so as to advance the understanding of those flow and transport processes for which network topology in not the key determinant.

Appendix A: Numbers of Nodes and Segments in the Peano Network

The Peano network having a generic order Ω can be constructed through the iterative procedure sketched in Figure 3. If we indicate with s_Ω and n_Ω the numbers of segments and nodes, respectively, in the Peano network having order Ω, we can easily obtain the recursive relations

$$s_{\Omega+1}=s_\Omega+3\,s_\Omega=4\,s_\Omega \tag{A1}$$

and

$$n_{\Omega+1}=n_\Omega+3s_\Omega, \tag{A2}$$

where $s_{\Omega+1}$ and $n_{\Omega+1}$ are the numbers of segments and nodes, respectively, in the Peano network having order $\Omega+1$. The number $n_\Omega^{(e)}$ of exterior nodes (including the source and outlet nodes) satisfies the recursive relation

$$n_{\Omega+1}^{(e)}=n_\Omega^{(e)}+2s_\Omega, \tag{A3}$$

whereas the number $n_\Omega^{(i)}$ of interior nodes satisfies the recursive relation

$$n_\Omega^{(i)}=n_{\Omega-1}^{(i)}+s_{\Omega-1}. \tag{A4}$$

Equations (A1)–(A4) are first-order linear difference equations that can be solved by incorporating the initial conditions $s_1=1$, $n_1=2$, $n_1^{(e)}=2$, and $n_2^{(i)}=1$ to give

$$s_\Omega=4^{\Omega-1}, \tag{A5}$$

$$n_\Omega=4^{\Omega-1}+1, \tag{A6}$$

$$n_\Omega^{(e)}=\frac{8}{3}(4^{\Omega-2}-1)+4, \tag{A7}$$

and

$$n_\Omega^{(i)}=\frac{1}{3}(4^{\Omega-1}-1), \tag{A8}$$

respectively [*Elaydi*, 2005]. The validity of equations (A5)–(A8) can be proved by using an induction on the order Ω.

Appendix B: Lengths of Segments in Peano Networks

As reported in section 2.4, the maximum order Ω of a Peano grid network is related to the exponent n in the grid domain size through the relation

$$\Omega=n+1. \tag{B1}$$

Therefore, Ω does not depend on the grid cell size h, but only on the grid domain size n. Differently, the lengths $L_\Omega^{(e)}$ and $L_\Omega^{(i)}$ of the exterior and interior segments, respectively, depend on the grid cell size h. These quantities are expressed by the relationships

$$L_\Omega^{(e)}=\frac{n_\Omega^{(e)}}{2}h\sqrt{2} \tag{B2}$$

and

$$L_\Omega^{(i)}=(n_\Omega^{(i)}-1)h\sqrt{2}, \tag{B3}$$

where $n_\Omega^{(e)}$ and $n_\Omega^{(i)}$ are given by equations (A7) and (A8), respectively. The total length $L_\Omega^{(T)}$ of segments of all orders is given by

$$L_{\Omega}^{(T)} = L_{\Omega}^{(e)} + L_{\Omega}^{(i)}, \tag{B4}$$

where $L_{\Omega}^{(e)}$ and $L_{\Omega}^{(i)}$ are given by equations (B2) and (B3), respectively.

As reported in section 2.4, Peano channel networks can be extracted from Peano grid networks by imposing a threshold on the drainage area A or on the Strahler order ω^*. The threshold value A_t can be expressed as

$$A_t = 4^m h^2, \tag{B5}$$

where the exponent m is a fixed integer between 1 and Ω. If m is fixed, then the maximum order Ω_C of the Peano channel network is obtained by the equation

$$\Omega_C = \Omega - m. \tag{B6}$$

The lengths $L_{\Omega_C}^{(e)}$ and $L_{\Omega_C}^{(i)}$ of the exterior and interior segments, respectively, are expressed by the relationships

$$L_{\Omega_C}^{(e)} = \frac{n_{\Omega_C}^{(e)}}{2} h\sqrt{2} + (2^m - 1)h\sqrt{2} \tag{B7}$$

and

$$L_{\Omega_C}^{(i)} = 2^m (n_{\Omega_C}^{(i)} - 1)h\sqrt{2}, \tag{B8}$$

where $n_{\Omega_C}^{(e)}$ and $n_{\Omega_C}^{(i)}$ are given by equations (A7) and (A8). The total length $L_{\Omega_C}^{(T)}$ of segments of all orders is given by

$$L_{\Omega_C}^{(T)} = L_{\Omega_C}^{(e)} + L_{\Omega_C}^{(i)}, \tag{B9}$$

where $L_{\Omega_C}^{(e)}$ and $L_{\Omega_C}^{(i)}$ are given by equations (B7) and (B8), respectively.

If the threshold value ω_t^* is fixed, then the maximum order Ω_C of the Peano channel network is obtained by the equation

$$\Omega_C = \Omega - \omega_t^*. \tag{B10}$$

The lengths $L_{\Omega_C}^{(e)}$ and $L_{\Omega_C}^{(i)}$ of the exterior and interior segments, respectively, are expressed by the relationships

$$L_{\Omega_C}^{(e)} = (2^{\omega_t^*} - 1/2) n_{\Omega_C}^{(e)} h\sqrt{2} \tag{B11}$$

and

$$L_{\Omega_C}^{(i)} = 2^{\omega_t^*} (n_{\Omega_C}^{(i)} - 1)h\sqrt{2}, \tag{B12}$$

where $n_{\Omega_C}^{(e)}$ and $n_{\Omega_C}^{(i)}$ are given by equations (A7) and (A8), respectively. The total length $L_{\Omega_C}^{(T)}$ of segments of all orders is given by

$$L_{\Omega_C}^{(T)} = L_{\Omega_C}^{(e)} + L_{\Omega_C}^{(i)}, \tag{B13}$$

where $L_{\Omega_C}^{(e)}$ and $L_{\Omega_C}^{(i)}$ are given by equations (B11) and (B12), respectively.

Acknowledgments
This study was carried out under the research program PRIN 2010-2011 (grant 2010JHF437) funded by the Italian Ministry of Education, University, and Research. The authors thank Taylor Perron (Massachusetts Institute of Technology, USA) for providing high-resolution digital elevation model data for the GM1 and AP1 drainage basins. The data in our article can be provided upon request to Samuele De Bartolo (samuele.debartolo@unical.it) or Giovanni Moretti (giovanni.moretti@unimore.it). The authors are grateful to Erkan Istanbulluoglu and three anonymous reviewers for comments that led to significant improvements in the manuscript.

References

Albert, R., and A. L. Barabási (2002), Statistical mechanics of complex networks, *Rev. Mod. Phys.*, *74*, 47–97.
Bertuzzo, E., A. Maritan, M. Gatto, I. Rodriguez-Iturbe, and A. Rinaldo (2007), River networks and ecological corridors: Reactive transport on fractals, migration fronts, hydrochory, *Water Resour. Res.*, *43*, W04419, doi:10.1029/2006WR005533.
Bertuzzo, E., S. Azaele, A. Maritan, M. Gatto, I. Rodriguez-Iturbe, and A. Rinaldo (2008), On the space-time evolution of a cholera epidemic, *Water Resour. Res.*, *44*, W01424, doi:10.1029/2007WR006211.
Bertuzzo, E., R. Casagrandi, M. Gatto, I. Rodriguez-Iturbe, and A. Rinaldo (2010), On spatially explicit models of cholera epidemics, *J. R. Soc. Interface*, *7*, 321–333.
Bras, R. L. (1990), *Hydrology: An Introduction to Hydrologic Science*, Addison-Wesley, Reading, Mass.
Camporese, M., C. Paniconi, M. Putti, and S. Orlandini (2010), Surface-subsurface flow modeling with path-based runoff routing, boundary condition-based coupling, and assimilation of multisource observation data, *Water Resour. Res.*, *46*, W02512, doi:10.1029/2008WR007536.

Campos, D., J. Fort, and V. Méndez (2006), Transport on fractal river networks: Application to migration fronts, *Theor. Popul. Biol.*, *69*, 88–93.
De Bartolo, S., F. Dell'Accio, and M. Veltri (2009), Approximations on the Peano river network: The case of low connections applying the Horton-Strahler hierarchy, *Phys. Rev. E*, *79*, 026108.
De Bartolo, S. G., S. Gabriele, and R. Gaudio (2000), Multifractal behaviour of river networks, *Hydrol. Earth Syst. Sci.*, *4*(1), 105–112.
De Bartolo, S. G., R. Gaudio, and S. Gabriele (2004), Multifractal analysis of river networks: Sandbox approach, *Water Resour. Res.*, *40*, W02201, doi:10.1029/2003WR002760.
De Bartolo, S. G., L. Primavera, R. Gaudio, A. D'Ippolito, and M. Veltri (2006a), Fixed-mass multifractal analysis of river networks and braided channels, *Phys. Rev. E*, *74*, 026101.
De Bartolo, S. G., L. Primavera, and M. Veltri (2006b), Estimated generalized dimensions of river networks, *J. Hydrol.*, *322*, 181–191, doi:10.1016/j.jhydrol.2005.02.033.
Dekking, F. M. (1991), Construction of fractals and dimension problems, in *Fractals: Non-Integral Dimensions and Applications*, edited by G. Cherbit, 94 pp., John Wiley, N. Y.
Dodds, P., and D. Rothman (1999), Unified view of scaling laws for river networks, *Phys. Rev. E*, *59*(5), 4865–4877.
Elaydi, S. N. (2005), *An Introduction to Difference Equations*, Springer, Berlin.
Flammini, A., and F. Colaiori (1996), Exact analysis of the Peano basin, *J. Phys. A: Math. Gen.*, *29*, 6701–6708.
Gaudio, R., S. G. De Bartolo, L. Primavera, S. Gabriele, and M. Veltri (2006), Lithologic control on the multifractal spectrum of river networks, *J. Hydrol.*, *327*, 365–375, doi:10.1016/j.jhydrol.2005.11.025.
Giusti, E., and W. J. Schneider (1965), The distribution of branches in river networks, *U.S. Geol. Surv. Prof. Pap.*, *422-G*, 10 pp.
Helmlinger, K., P. Kumar, and E. Foufoula-Georgiou (1993), On the use of digital elevation model data for Hortonian and fractal analyses of channel networks, *Water Resour. Res.*, *29*(8), 2599–2613.
Horton, R. E. (1932), Drainage basin characteristics, *Eos Trans. AGU*, *13*, 350–361.
Horton, R. E. (1945), Erosional development of streams and their drainage basins: Hydrophysical approach to quantitative morphology, *Geol. Soc. Am. Bull.*, *56*(3), 275–370.
Howard, A. D. (1971), Optimal angles of stream junction: Geometric, stability to capture, and minimum power criteria, *Water Resour. Res.*, *7*(4), 863–873.
Howard, A. D. (1990), Theoretical model of optimal drainage networks, *Water Resour. Res.*, *26*(9), 2107–2117.
Kirchner, J. W. (1993), Statistical inevitability of Horton's laws and the apparent randomness of stream channel networks, *Geology*, *21*, 591–594.
La Barbera, P., and R. Rosso (1989), On the fractal dimension of steam networks, *Water Resour. Res.*, *25*(4), 735–741.
Mandelbrot, B. (1977), *Fractals: Form, Chance and Dimension*, 365 pp., W. H. Freeman, N. Y.
Marani, A., R. Rigon, and A. Rinaldo (1991), A note on fractal channel networks, *Water Resour. Res.*, *27*(12), 3041–3049.
Montgomery, D. R., and J. M. Buffington (1997), Channel-reach morphology in mountain drainage basins, *Geol. Soc. Am. Bull.*, *109*(5), 596–611.
Montgomery, D. R., and W. E. Dietrich (1988), Where do channels begin?, *Nature*, *336*(6196), 232–234.
Newman, M. E. J. (2003), The structure and function of complex networks, *SIAM Rev.*, *45*, 167–256.
O'Callaghan, J., and D. M. Mark (1984), The extraction of drainage networks from digital elevation data, *Comput. Vis. Graph. Image Processes*, *28*(3), 323–344.
Orlandini, S., and G. Moretti (2009), Determination of surface flow paths from gridded elevation data, *Water Resour. Res.*, *45*, W03417, doi:10.1029/2008WR007099.
Orlandini, S., G. Moretti, M. Franchini, B. Aldighieri, and B. Testa (2003), Path-based methods for the determination of nondispersive drainage directions in grid-based digital elevation models, *Water Resour. Res.*, *39*(6), 1144, doi:10.1029/2002WR001639.
Orlandini, S., P. Tarolli, G. Moretti, and G. Dalla Fontana (2011), On the prediction of channel heads in a complex alpine terrain using gridded elevation data, *Water Resour. Res.*, *47*, W02538, doi:10.1029/2010WR009648.
Orlandini, S., G. Moretti, and A. Gavioli (2014), Analytical basis for determining slope lines in grid digital elevation models, *Water Resour. Res.*, *50*, 526–539, doi:10.1002/2013WR014606.
Peckham, S. D. (1995a), Self-similarity in the three-dimensional geometry and dynamics of large river basins, PhD thesis, Univ. of Colorado, Boulder.
Peckham, S. D. (1995b), New results for self-similar trees with applications to river networks, *Water Resour. Res.*, *31*(4), 1023–1029.
Perron, J. T., P. W. Richardson, K. L. Ferrier, and M. Lapôtre (2012), The root of branching river networks, *Nature*, *492*, 100−104, doi:10.1038/nature11672.
Pirotti, F., and P. Tarolli (2010), Suitability of LiDAR point density and derived landform curvature maps for channel network extraction, *Hydrol. Processes*, *24*(9), 1187–1197, doi:10.1002/hyp.7582.
Rigon, R., A. Rinaldo, I. Rodriguez-Iturbe, E. Ijjasz-Vasquez, and R. L. Bras (1993), Optimal channel networks: A framework for the study of river basin morphology, *Water Resour. Res.*, *29*(6), 1635–1646.
Rinaldo, A., I. Rodriguez-Iturbe, R. Rigon, R. L. Bras, E. Ijjasz-Vasquez, and A. Marani (1992), Minimum energy and fractal structures of drainage networks, *Water Resour. Res.*, *28*(9), 2183–2195.
Rinaldo, A., I. Rodriquez-Iturbe, and R. Rigon (1998), Channel networks, *Annu. Rev. Earth Planet. Sci.*, *26*, 289–327.
Rinaldo, A., J. R. Banavar, and A. Maritan (2006), Trees, networks, and hydrology, *Water Resour. Res.*, *42*, W06D07, doi:10.1029/2005WR004108.
Rodriguez-Iturbe, I., and A. Rinaldo (1997), *Fractal River Networks: Chance and Self-Organization*, 547 pp., Cambridge Univ. Press, New York.
Shreve, R. L. (1966a), Statistical law of stream numbers, *J. Geol.*, *74*, 17–37.
Shreve, R. L. (1966b), Stream lengths and basin areas in topologically random channel networks, *J. Geol.*, *77*, 397–414.
Shreve, R. L. (1967), Infinite topologically random channel networks, *J. Geol.*, *75*, 178–186.
Sibson, R. (1981), A brief description of natural neighbor interpolation, in *Interpreting Multivariate Data*, edited by V. Barnett, pp. 21–36, John Wiley, Chichester.
Strahler, A. N. (1952), Hypsometric (area-altitude) analysis of erosional topology, *Geol. Soc. Am. Bull.*, *63*(11), 1117–1142.
Strahler, A. N. (1957), Quantitative analysis of watershed geomorphology, *Trans. AGU*, *8*(6), 913–920.
Strahler, A. N. (1958), Dimensional analysis applied to fluvially eroded landforms, *Geol. Soc. Am. Bull.*, *69*, 279–300.
Tarboton, D. G. (1997), A new method for the determination of flow directions and upslope areas in grid digital elevation models, *Water Resour. Res.*, *33*(2), 309–319.
Tarboton, D. G., R. L. Bras, and I. Rodriguez-Iturbe (1988), The fractal nature of river networks, *Water Resour. Res.*, *24*(8), 1317–1322.
Tarboton, D. G., R. L. Bras, and I. Rodriguez-Iturbe (1991), On the extraction of channel networks from digital elevation data, *Hydrol. Processes*, *5*, 81–100.

Tay, L. T., B. S. D. Sagar, and H. T. Chuah (2006), Allometric relationships between traveltime channel networks, convex hills, and convexity measures, *Water Resour. Res.*, *42*, W06502, doi:10.1029/2005WR004092.

Taylor, J. R. (1997), *An Introduction to Error Analysis: The Study of Uncertainties in Physical Measurements*, Univ. Sci. Books, Sausalito, Calif.

Troutman, B. M., and T. M. Over (2001), River flow mass exponents with fractal channel networks and rainfall, *Adv. Water Resour.*, *24*, 967–989.

Tucker, G. E., F. Catani, A. Rinaldo, and R. L. Bras (2001), Statistical analysis of drainage density from digital terrain data, *Geomorphology*, *36*(3–4), 187–202.

Veitzer, S. A., and V. K. Gupta (2001), Statistical self-similarity of width function maxima with implications to floods, *Adv. Water Resour.*, *24*, 955–965.

Veneziano, D., G. E. Moglen, P. Furcolo, and V. V. Iacobellis (2000), Stochastic model of the width function, *Water Resour. Res.*, *36*(4), 1143–1157.

Willgoose, G., R. L. Bras, and I. Rodriguez-Iturbe (1991a), Results from a new model of river basin evolution, *Earth Surf. Processes Landforms*, *16*, 237–254.

Willgoose, G., R. L. Bras, and I. Rodriguez-Iturbe (1991b), A coupled channel network growth and hillslope evolution model: 1. Theory, *Water Resour. Res.*, *27*(7), 1671–1684.

Willgoose, G., R. L. Bras, and I. Rodriguez-Iturbe (1991c), A coupled channel network growth and hillslope evolution model: 2. Nondimensionalization, *Water Resour. Res.*, *27*(7), 1685–1696.

Willgoose, G., R. L. Bras, and I. Rodriguez-Iturbe (1991d), A physical explanation of an observed link area-slope relationship, *Water Resour. Res.*, *27*(7), 1697–1702.

Yang, D., S. Herath, and k. Musiake (2001), Spatial resolution sensitivity of catchment geomorphologic properties and the effect on hydrological simulation, *Hydrol. Processes*, *15*, 2085–2099.